

Secretory Portal-*Porosome* in Pancreatic Acinar Cells

Bhanu P. Jena

Department of Physiology, Wayne State University School of Medicine, Detroit, MI 48201,
USA.

e-mail: bjena@med.wayne.edu

Version 2.0, February 5th, 2021. DOI: [[10.3998/panc.2021.04](https://doi.org/10.3998/panc.2021.04)]

I. INTRODUCTION

Secretion is a fundamental process through which cells communicate with their environment and exchange information in a multicellular context to reach homeostasis and sustain life. For decades, the prevailing view was that secretion operates as an all-or-none 'complete fusion' event, where vesicles are trafficked to the cell surface to fuse and completely incorporate into the plasma membrane. The vesicle contents then diffuse out of the cell. This hypothesis, although attractive at first glance, had several key setbacks. First, it predicted a quantization of secretory products packaged into each secretory vesicle, when in fact, secretory vesicle size greatly varies even within the same cell, sometimes as much as 6-fold. Second, the level of additional regulation necessary to rapidly and precisely internalize and sequester vesicle-associated lipids and proteins following incorporation into the cell plasma membrane seem extraordinarily complex, given the tens of thousands of different membrane lipids and their differential distribution even between the same bilayer leaflets. Third, following a secretory episode, partially empty secretory vesicles accumulate within cells as observed in electron micrographs (**Figure 1**), demonstrating that secretory vesicles are capable of transient fusion at the cell plasma membrane and incomplete or partial content release.

We therefore hypothesized some 25 years ago, the presence of a tunable dial at the cell plasma membrane for secretory vesicle docking and fusion without full collapse, and the generation of hydrostatic pressure within vesicles to drive vesicular contents to the cell exterior. Through the use of atomic force microscope, a force spectroscope, we identified nanoscale transmembrane cup-shaped lipoprotein structures at the cell plasma membrane first in acinar cells of the exocrine pancreas, and later in all cells examined including neurons. We named the structures 'porosomes,' that have since been implicated in a wide range of secretory events. The family of proteins that make up the porosome has been biochemically identified and the mesoscale structure of the complex has been well characterized through electron microscopy and solution X-ray methods. Defects in one or more porosome components has measurable, often highly potent effects on the regulation of secretion, establishing links between point mutations and secretion-defective disease states such as neurological disorders and cystic fibrosis that were previously correlative and are now causative. The discovery of the porosome solved the conundrum of fractional discharge of intravesicular contents from cells by providing an explanation for regulated graded secretion. Porosomes are cup-shaped unidirectional (inside cells to the outside) transport

machineries, which are supramolecular lipoprotein structures at the cell plasma membrane ranging in size from 15 nm in neurons, to 100-180 nm in endocrine and exocrine cells and composed of around 30-40 proteins. In comparison, the 120 nm bidirectional transport machinery, the nuclear pore complex is composed of nearly 1,000 protein molecules.

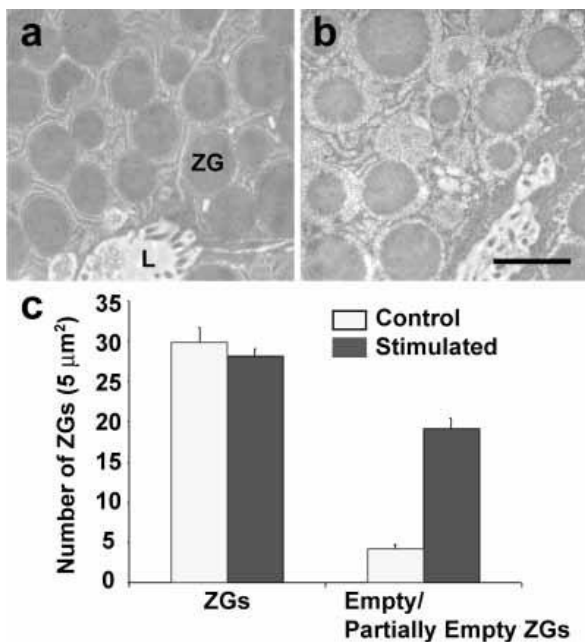


Figure 1. Partial emptying of zymogen granules in acinar cells of the rat exocrine pancreas following secretion. Representative electron micrographs of resting (a), and cholecystokinin-stimulated for 15 min (b) rat pancreatic acinar cells, demonstrating partial loss of zymogen granule (ZG) contents following secretion. The apical lumen (L) of acini demonstrating the presence of microvilli and secreted products is observed. (c) These studies using electron microscopy further demonstrate that while the number of ZG remain unchanged following secretion, an increase in the number of empty and partially empty vesicles are observed. Scale bar = 1 μm. (From reference (10)).

Porosomes in the exocrine pancreas will be the major focus in this article

In 1973, the ‘transient’ or ‘kiss-and-run’ mechanism of secretory vesicle fusion at the cell plasma membrane enabling fractional release of intravesicular contents during secretion, was proposed (7). Nearly two decades later in 1990, it was hypothesized that the fusion pore, a continuity established between the vesicle membrane and

the cell plasma membrane, results from a “preassembled ion channel-like structure that could open and close” (2). A later 1992 review (56) opined that the principal difficulty in observing these hypothetical pore structures, was the lack of ultrahigh resolution imaging tools to directly monitor their presence and study their activity in live cells.

In the mid 1990’s, employing the then newly developed technique of atomic force microscopy (AFM), nanometer-scale cup-shaped pore structures and their dynamics were discovered at the apical plasma membrane in live pancreatic acinar cells (62). Circular pit-like structures containing 100-180 nm cup-shaped depressions or pores were observed at the apical plasma membrane of pancreatic acinar cells where secretion is known to occur (62). During secretion, the depression or pore openings grew larger, returning to their resting size following completion of cell secretion.

Studies next established the observed depressions to be the secretory portals at the cell plasma membrane (13, 36). Following stimulation of secretion, gold-conjugated amylase antibodies (amylase being one of the major intra-vesicular enzymes secreted by pancreatic acinar cells) accumulate at depressions. These results established depressions to be the long sought-after secretory portals in cells. The study further reported (36) the presence of t-SNAREs at the porosome base facing the cytosol, firmly establishing depression structures to be secretory portals where zymogen granules (ZGs) transiently dock and fuse for intra-vesicular content release during secretion (36). Subsequently porosomes and their dynamics at the cell plasma membrane in growth hormone (GH) secreting cells of the pituitary gland, and in rat chromaffin cells (15) was reported. In 2003, following immunoisolation of the porosome structures from acinar cells of the exocrine pancreas, its composition was determined, and isolated porosomes were functionally reconstituted into artificial lipid membranes (42). Morphological details of

porosome associated with docked secretory vesicles were revealed using high-resolution electron microscopy (42). In the past decade, employing a combination of approaches such as AFM, biochemistry, electrophysiology, conventional EM, mass spectrometry, and small angle X-Ray solution scattering analysis, this specialized secretory portal has been extensively characterized and documented, and found to be present in all cells examined, including neurons (18, 37, 48). Studies (11,13,15,18,21,23,24,27-29,33-38,42,48,52,59,61,62,68,74,82) establish porosomes to be secretory portals that perform the specialized task of fractional discharge of intravesicular contents from cells during secretion. The porosome structure and the associated transient fusion mechanism (3,73,75) accompanied by fractional discharge of vesicular contents from cells, has greatly progressed in the past two decades. It has been demonstrated in

exocrine, endocrine, and neuronal cells that “secretory granules are recaptured largely intact following stimulated exocytosis in cultured endocrine cells” (73); that “single synaptic vesicles fuse transiently and successively without loss of identity” (3); and that “zymogen granule exocytosis is characterized by long fusion pore openings and preservation of vesicle lipid identity” (48, 75). The past two decades have additionally witnessed much progress in our understanding of Ca^{2+} and SNARE-mediated membrane fusion (4, 6, 8, 12, 16, 17, 20, 22, 25, 30-32, 39, 41, 43, 53, 55, 58, 60, 64, 66, 69, 70-73,79-81) and on secretory vesicle volume regulation required for precise fractional release of intravesicular contents from cells (9, 14, 35, 40, 44, 50, 65) during secretion. These findings have greatly contributed to the progress in our understanding of porosome-mediated fractional release of intravesicular contents from cells during secretion.

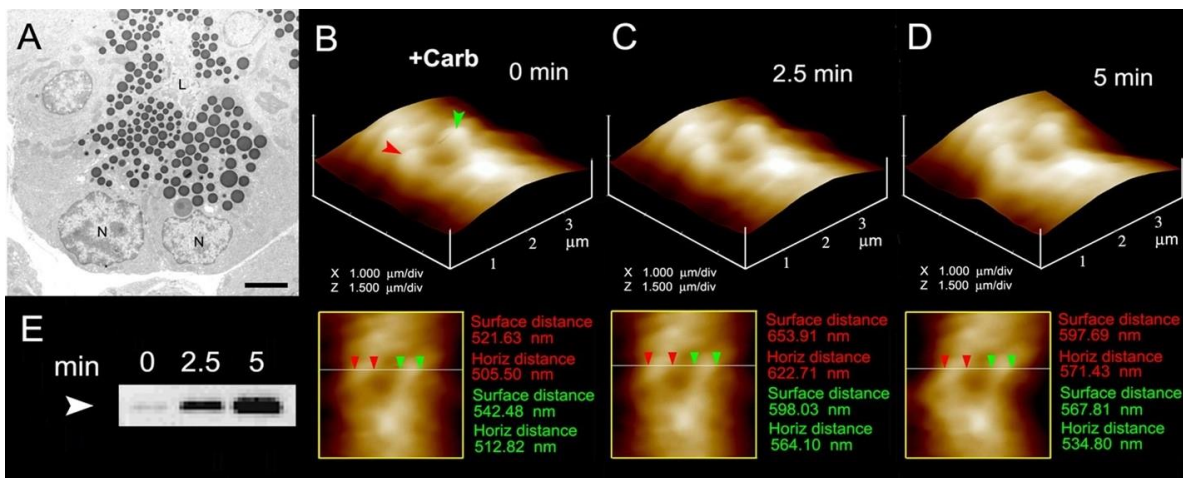


Figure 2. The volume dynamics of zymogen granules (ZG) in live pancreatic acinar cells demonstrating fractional release of ZG contents during secretion. (A) Electron micrograph of pancreatic acinar cells showing the basolaterally located nucleus (N) and the apically located electron-dense vesicles, the ZGs. The apical end of the cell faces the acinar lumen (L). Bar = 2.5 μm . **(B-D)** Apical ends of live pancreatic acinar cells in physiological buffer imaged by AFM, showing ZGs (red and green arrowheads) lying just below the apical plasma membrane. Exposure of the cell to a secretory stimulus (1 μM carbamylcholine), results in ZG swelling within 2.5 min, followed by a decrease in ZG size after 5 min. The decrease in size of ZGs after 5 min is due to the release of secretory products such as α -amylase, as demonstrated by the immunoblot assay in **(E)**. If ZG's had fused at the plasma membrane and fully merged, it would not be visible, demonstrating transient fusion and fractional discharge on intravesicular contents during secretion in pancreatic acinar cells. (From reference (44)).

II. Porosome Discovery: AFM Trained on Pancreatic Acini

As noted earlier, the porosome was first discovered in acinar cells of the rat exocrine pancreas nearly

25 years ago (62). This discovery was made possible by the use of a then new microscope, the AFM (1,5). In AFM, a probe tip micro fabricated from silicon or silicon nitride and mounted on a cantilever spring is used to scan the surface of the

sample at a constant force. Either the probe or the sample can be precisely moved in a raster pattern using a xyz piezo to scan the surface of the sample. The deflection of the cantilever measured optically is used to generate an isoforce relief of the sample (1, 5). Force is thus used by the AFM to image surface profiles of objects at nanometer resolution and in real time, objects such as live cells, subcellular organelles, and even biomolecules, submerged in physiological buffer solutions.

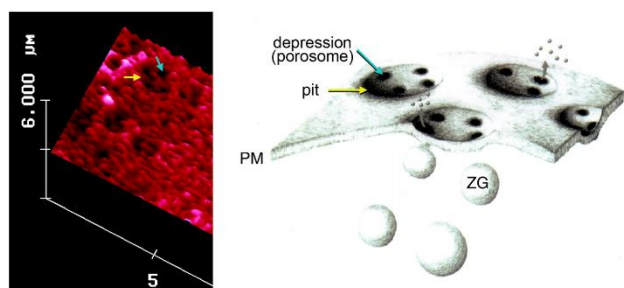


Figure 3. To the left is an AFM micrograph of the apical plasma membrane of a live pancreatic acinar cell demonstrating the presence of a pit (yellow arrow) with depressions or porosomes within (blue arrow). To the right is a schematic drawing demonstrating pits and cup-shaped porosomes where zymogen granules (ZG), the secretory vesicles in exocrine pancreas dock and transiently fuse to release intra-vesicular digestive enzymes from the cell. (From reference (62)).

Compared to neurons and neuroendocrine cells, exocrine pancreas are slow secretory cells, secreting digestive enzymes over a period of minutes following a meal, as opposed to milliseconds or seconds in a fast secretor such as neurons and endocrine cells. Hence, pancreatic acinar cells were ideal for the discovery of possible plasma membrane structures that could be involved in the fractional release of intravesicular contents from cells during secretion. Similar to neurons, exocrine pancreatic acinar cells are polarized secretory cells possessing an apical and a basolateral end. Digestive enzymes in pancreatic acinar cells are stored within 0.2-1.2 μm in diameter apically located membrane-bound secretory vesicles, called zymogen granules (ZGs). It had been well established that following a secretory stimulus, ZGs dock and fuse at the apical plasma membrane to release their contents. The AFM was therefore trained at the apical plasma

membrane of live acinar cells in buffer, before and following stimulation of secretion. These studies demonstrate the presence of pore structures only at the apical plasma membrane of the cell where secretion is known to occur (62). A group of circular ‘pits’ measuring 0.4–1.2 μm in diameter, contain smaller 100-180 nm in diameter ‘depressions’ structures are identified (**Figure 3**). Typically 3–4 depressions are found within each pit structure. Basolateral membrane of acinar cells is devoid of such pit and depression structures (62). High-resolution AFM images of depressions in live acinar cells further reveal a cup-shaped basket-like morphology, each cup measuring 35 nm in depth and 100-180 nm in diameter. View of the porosome structure at the cytosolic compartment of the plasma membrane in pancreatic acinar cells has also been determined at near nm resolution (42) (**Figure 4**).

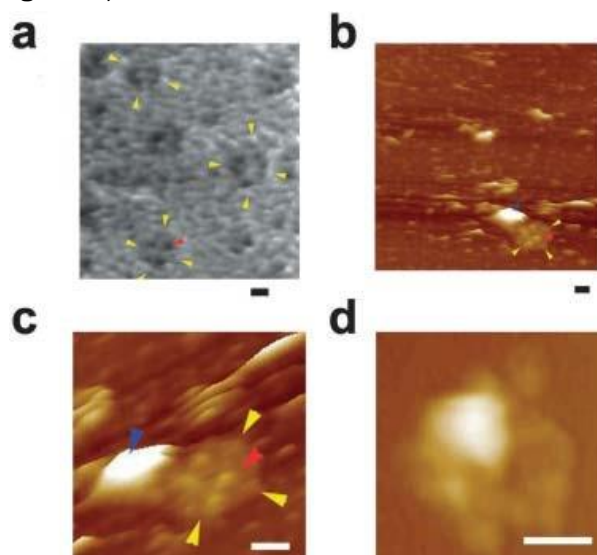


Figure 4. AFM micrograph showing cup-shaped depression or porosome structures at the pancreatic acinar cell plasma membrane. (a) Several circular “pits” (yellow arrowheads) with depressions or porosomes (red arrowheads) are seen in this AFM micrograph of the apical plasma membrane in live pancreatic acinar cell. (b) AFM micrograph of the cytosolic compartment of isolated pancreatic plasma membrane preparation depicting a “pit” (yellow arrowheads) containing several inverted cup-shaped porosomes (red arrowhead) within. ZG (blue arrowhead) is found associated with porosomes in figures c and d. (c) The “pit” and inverted fusion pores in b is shown at higher magnification. (d) AFM micrograph of another “pit” with inverted fusion pores within, and associated with a ZG, is shown. Bar = 200 nm. (From reference (42)).

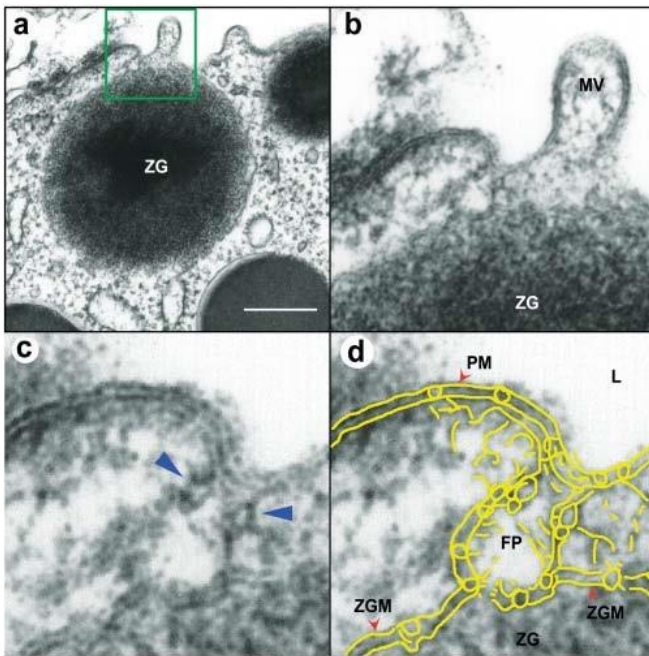


Figure 5. Transmission electron micrograph of a porosome associated with a docked secretory vesicle at the apical end of a pancreatic acinar cell. (a) Part of the apical end of a pancreatic acinar cell demonstrating within the green square, the presence of a porosome and an associated zymogen granule (ZG) fused at its base. (Bar=400 nm only in figure a). (b) The area within the green square in figure a, has been enlarged to show the apical microvilli (MV) and a section through the porosome and the ZG. Note the ZG membrane (ZGM) bilayer is fused at the base of the porosome cup. (c) A higher magnification the porosome-associated ZG shows in greater detail the porosome bilayer and cross section through the three protein rings (which appear as knobs in either side of the cup-shaped porosome), with the thicker ring (blue arrowhead) present close to the opening of the porosome to the outside, which may regulate the closing and opening of the structure. The third and the lowest ring away from the porosome opening is attached to the ZGM, and may represent the t-/v-SNARE rosette or ring complex. (d) Yellow outline of the ZG fused porosome complex (FP) demonstrating the continuity with the apical plasma membrane (PM) at the apical end of the pancreatic acinar cell facing the lumen (L). The exact points of contact and fusion of the ZGM with the membrane at the porosome base is clearly seen in the micrograph. (From reference (42)).

When isolated plasma membrane preparations of pancreatic acinar cells in near physiological buffered solution are imaged at ultrahigh resolution using the AFM, inverted cup-shaped structures, some with docked ZGs are demonstrated (42) (Figure 4). AFM surface topology maps of inside-out acinar cell plasma membrane preparations

reveal scattered circular disks (pits) measuring 0.5–1 μm in diameter, with inverted cup-shaped structures (depressions or porosomes) within (42). On a number of occasions, ZGs ranging in size from 0.4–1 μm in diameter are observed to be docked at the base of one or more porosomes (40) (Figure 4). These results further demonstrated that a single secretory vesicle may dock at more than one porosome at the cell plasma membrane. Porosomes in acinar cells of the exocrine pancreas have also been examined using high-resolution transmission electron microscopy (TEM) (Figures 5 and 6), both in isolated cells and tissues (Figure 5), and in association with ZGs prepared from stimulated acinar cells (Figure 6) (21, 36, 42, 74). In Figure 5, the electron micrograph of a porosome sectioned at a certain angle, reveals its distinct and separate bilayer, and the bilayer membrane attachment of the associated ZG. A cross section through three lateral knob-like structures that circle around the porosome cup, are clearly delineated. The apical knob-like density at the lip of the porosome, appear most prominent, and is hypothesized to be composed of actin and myosin, involved in the dilation of the porosome opening during cell secretion. The TEM micrograph further suggests that the lower knob, likely representing the t-/v-SNARE ring or rosette complexes formed as a consequence of ZG docking and fusion at the base of the porosome complex. Elegant TEM studies in the exocrine pancreas by Craciun and Barbu-Tudoran report docked and post-docked or dissociated ZGs (21). Similarly, secretory vesicles at the porosome base have been reported at the nerve terminal (44,48,32) and the arrangement of the SNARE complex in a ring or rosette conformation at the porosome base demonstrated (16). As previously outlined, invitro studies further reveal the Ca^{2+} and SNARE-mediated membrane fusion to establish the fusion pore (4, 6, 8, 12, 16, 17, 20, 22, 25, 30-32, 39, 41, 43, 53, 55, 58, 60, 64, 66, 67,69, 70-73,79-81) and the molecular process of secretory vesicle volume regulation required for the precise fractional release of intravesicular contents from cells (9, 14, 35, 40, 44, 50, 65) during secretion.

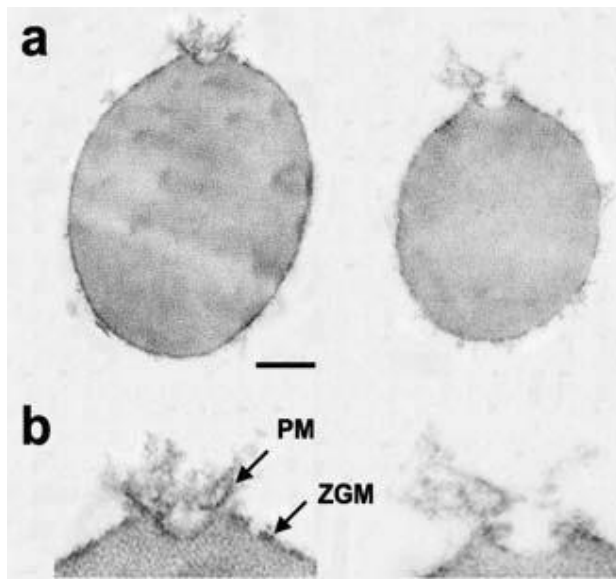


Figure 6. Transmission electron micrographs of zymogen granules (ZGs) co-isolated with porosomes. (a) Porosome associated at the surface of ZGs are shown. (Bar=120 nm; top panel only). (b) At higher magnification details of the porosome complex demonstrating the presence of separate plasma membrane (PM) and the ZG membrane (ZGM). Note the apically arranged ring complex of the porosome, similar to what is observed in electron micrographs of the structure in intact cells as presented in figure 5. These ZG-associated porosomes are torn off the cell plasma membrane and hence have very little membrane. Hence the porosome proteins lining the porosome cup appear as frills in the electron micrograph. Note the ZG size compared to the porosome structure. (From reference 42).

Exposure of pancreatic acinar cells to a secretory stimulus, results in a time-dependent increase (20–45%) in both the diameter and relative depth of porosomes (Figure 7). Porosomes return to their resting size on completion of cell secretion (13, 62). No demonstrable change in pit size is detected following stimulation of secretion (62). Enlargement of porosome diameter and an increase in its relative depth, following exposure to a secretory stimulus correlates with secretion (Figures 7 and 8). Additionally, exposure to cytochalasin B, a fungal toxin that inhibits actin polymerization and secretion, results in a 15–20% decrease in porosome size and a consequent 50–60% loss in cell secretion (62). These results suggested depressions or porosomes to be the secretory portals in pancreatic acinar cells. Results from these studies further demonstrate actin to compose the porosome in addition to implicating

actin in regulation of both the structure and function of porosomes. To further demine if porosomes serve as cellular secretory portals, the direct observation of the release of secretory products through the structure was required. This was accomplished using immuno-AFM studies in acinar cells of the exocrine pancreas (13) (Figures 9 and 10) where gold-conjugated amylase-specific antibody was demonstrated to selectively decorate the porosome opening following a secretory stimulus (13, 36).

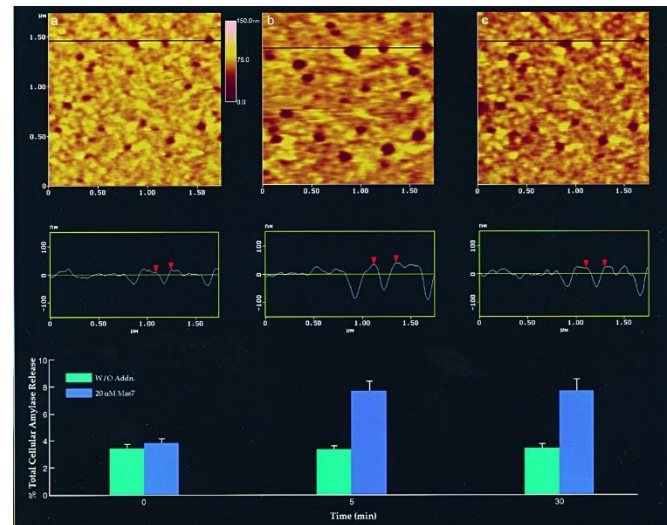


Figure 7. Dynamics of porosomes following stimulation of secretion in live pancreatic acinar cell examined using AFM. (a) Several porosomes within a pit are shown in the AFM micrographs. The scan line across three porosomes in the top panel is represented graphically in the middle panel and defines the diameter and relative depth of three porosomes. The porosome at the center, is labeled using red arrowheads. The bottom panel shows the percent total cellular amylase release in the presence (blue bars) and absence (green bars) of the secretion stimulatory tetradecapeptide mastoparan Mas7. (b) Note the increase in porosome diameter and relative depth, correlating with an increase in total cellular amylase release at 5 min following stimulation of secretion. (c) At the 30 min time point following stimulation, there is a decrease in diameter and depth of porosomes, with no further increase in amylase release following what is observed following the 5-min time point. No significant changes in amylase secretion or porosome size were observed in control acini, in either the presence or the absence of the non-stimulatory mastoparan analogue Mas17, throughout the time points examined. High-resolution images of both pits and their porosomes were obtained before and after stimulation with Mas7, for up to 30 min. (From reference (62)).

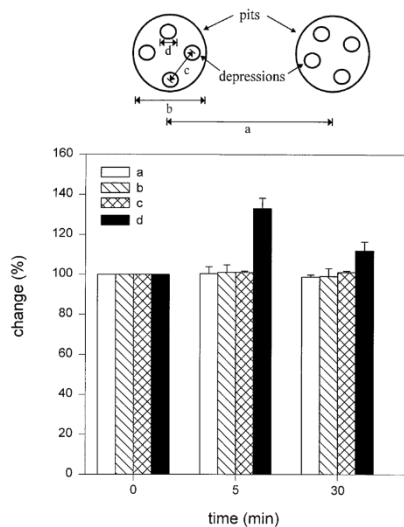


Figure 8. Changes are observed only in depressions or porosomes following stimulation of secretion. Analysis of the dimensions *a–d*, schematically represented at the top and graphically presented below, demonstrates a significant increase in the porosome diameter at 5 min and a return toward prestimulatory levels after 30 min. No changes (100%) in *a–c* are seen throughout the times examined. Pit and porosome diameters were estimated using section analysis software from Digital Instruments. Each single pit and porosome was measured twice, once in the scan direction and once at 90° to the first. (From reference (62)).

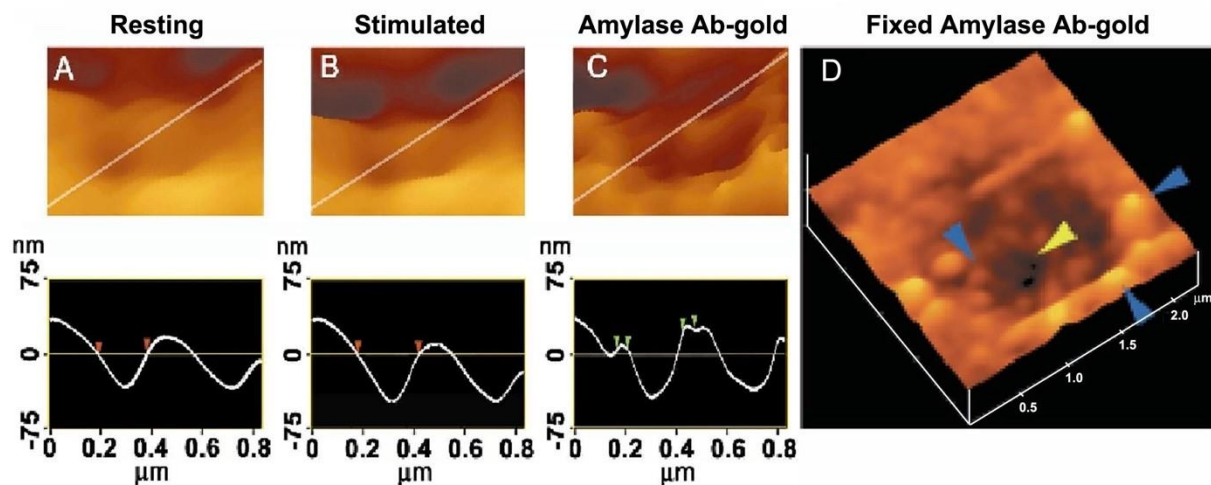


Figure 9. Intravesicular contents are expelled from within cells to the outside through the porosome during cell secretion. (A) and (B) AFM micrograph and section analysis of a pit and two of the four porosomes, demonstrating enlargement of porosomes following stimulation of cell secretion in the acinar cell of the exocrine pancreas. (C) Exposure of live cells to gold conjugated-amylase antibody (Ab) results in selective localization of gold particles to these secretory sites. Note the localization of amylase-specific 30 nm immunogold particles at the edge of porosomes. (D) AFM micrograph of pits and porosomes with immunogold localization demonstrated in cells immunolabeled and then fixed. Blue arrowheads point to immunogold clusters and the yellow arrowhead points to a porosome opening. (From reference (13)).

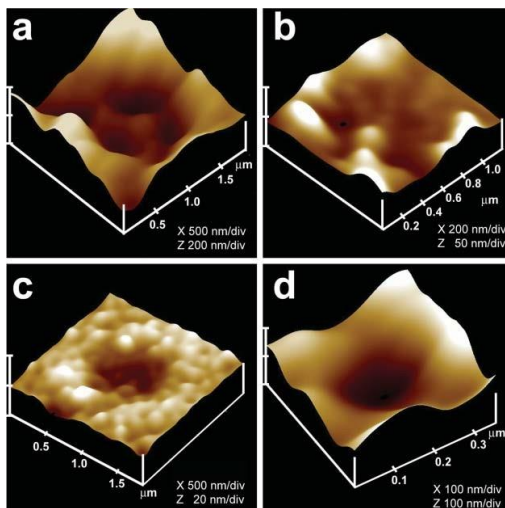


Figure 10. AFM and immune-AFM micrographs of the pancreatic acinar cell porosome demonstrating pore morphology and the release of secretory products at the site. (a) A pit with four porosomes within, found at the apical surface in a live pancreatic acinar cell; (b) After stimulation of secretion, amylase-specific immunogold localize at the pit and porosome openings, demonstrating porosomes to represent the secretory release sites in cells; (c) Some porosomes demonstrate greater immunogold localization, suggesting greater secretory product release through them; (d) AFM micrograph of a single porosome in a live acinar cell. (From reference (36)).

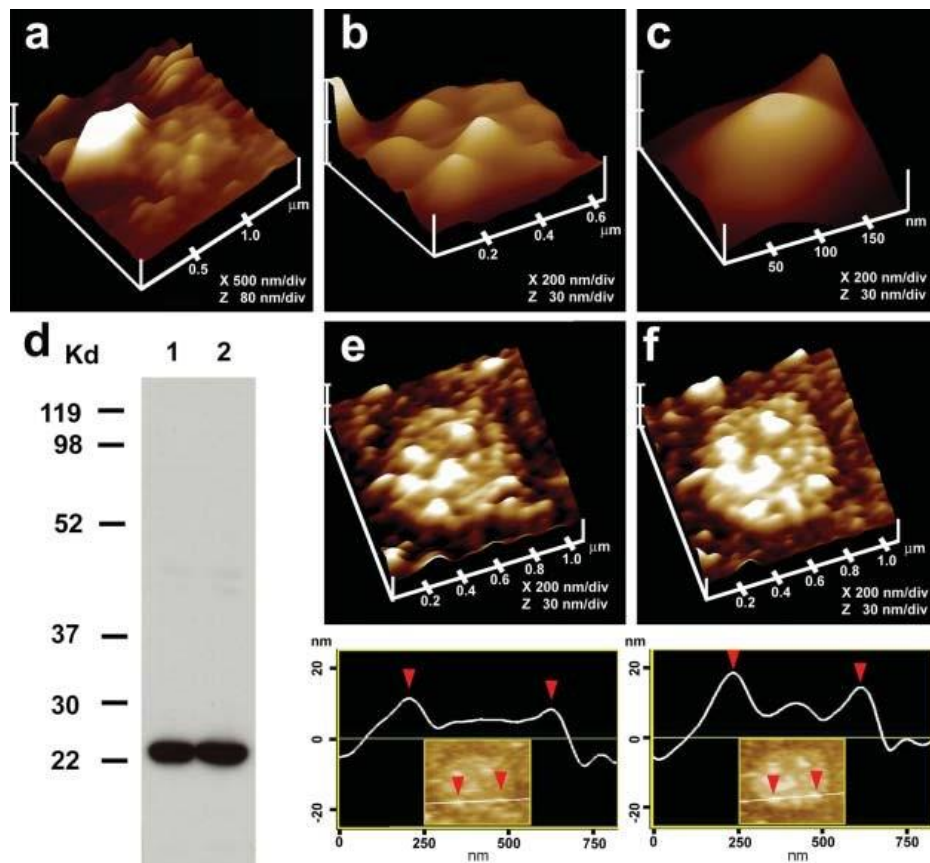


Figure 11. Immuno-AFM of the cytosolic compartment of the porosome complex demonstrate the presence of the t-SNARE protein SNAP-23 at the porosome base in acinar cell of the exocrine pancreas. (a) AFM micrograph of isolated plasma membrane preparation reveals the cytosolic compartment of a pit with inverted cup-shaped porosomes. Note the 600 nm in diameter docked ZG to the left. (b) Higher magnification of the same pit demonstrates the presence of 4–5 porosomes within. (c) A single porosome is depicted in this AFM micrograph. (d) Western blot analysis of 10 µg and 20 µg of pancreatic plasma membrane preparation resolved using SDS-PAGE, demonstrates a single 23kDa immunoreactive band when probed with SNAP-23-specific antibody. The over exposure of the film is to demonstrate the absence of no other bands, hence specificity of the antibody. (e) and (f) The cytosolic compartment of the plasma membrane with a pit having a number of porosomes within (e), demonstrate binding of the SNAP-23 specific antibody (f), establishing them to represent the docking sites of secretory vesicles at the cell plasma membrane. Note the increase in height of the porosome base revealed by section analysis (bottom panel), demonstrating localization of SNAP-23 antibody to the porosome base. (From reference (36)).

To further confirm that the cup-shaped structures are porosomes, where secretory vesicles dock and fuse, additional immuno-AFM studies have been performed (36). Since ZGs dock and fuse at the plasma membrane to release vesicular contents, it was hypothesized that if the inverted cups or porosomes are indeed the secretory portals, then plasma membrane-associated t-SNAREs should be present at the base of the porosome cup facing the cytosol. Since the t-SNARE protein SNAP-23 is present in pancreatic acinar cells (36), a polyclonal monospecific SNAP-23 specific antibody

recognizing a single 23 kDa protein in Western blots of pancreatic acinar cell plasma membrane fraction, was used in the study. Immuno-AFM studies demonstrate the selective binding of the SNAP-23 antibody to the base of the porosome complex (**Figure 11**) (36). These results establish that the inverted cup-shaped structures in the inside-out pancreatic plasma membrane preparations are indeed secretory portals or porosomes, where secretory vesicles transiently dock and fuse to release their contents during cell secretion.

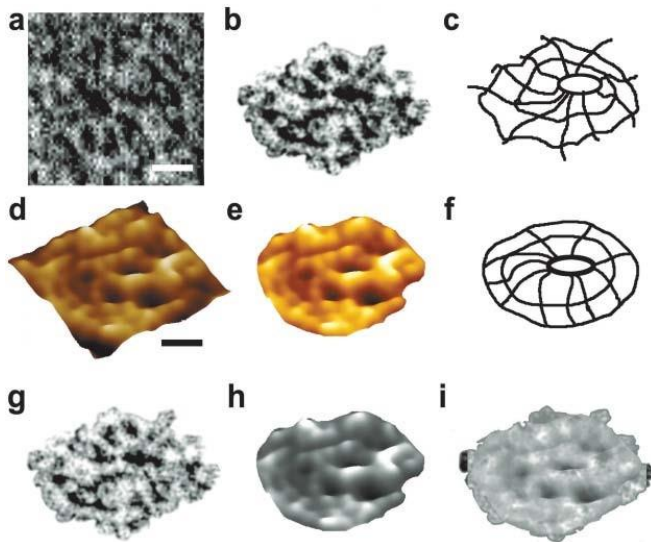


Figure 12. Negatively stained EM and AFM of the immunisolated porosome complex from exocrine pancreas. (a) Negatively stained EM of an immunisolated porosome complex from solubilized pancreatic plasma membrane preparation using a SNAP-23 specific antibody. Note the three rings and the 10 spokes that originate from the inner ring. This structure represents the protein backbone of the pancreatic porosome complex. Bar=30 nm. (b) EM of the isolated porosome complex extracted from figure a, and (c) an outline of the structure presented for clarity. (d–f) AFM micrograph of an isolated porosome complex in physiological buffer solution. Bar=30 nm. Note the structural similarity of the complex when imaged either by EM (g) or AFM (h). The EM and AFM micrographs are superimposable (i). (From reference (42)).

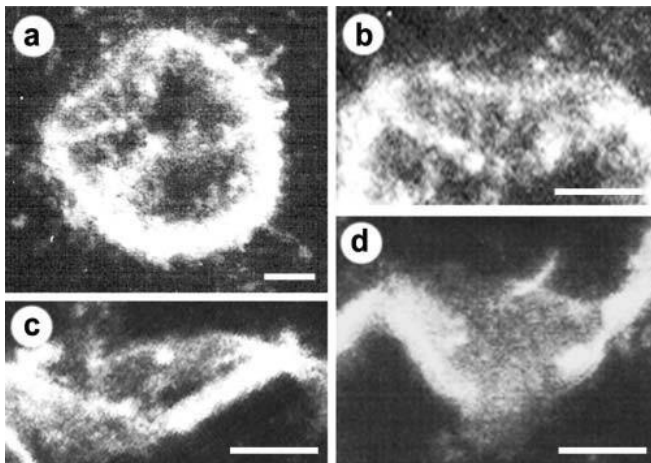


Figure 13. Electron micrographs of reconstituted porosome complex into liposomes, demonstrate a cup-shaped basket-like morphology. (a) A 500-nm vesicle with an incorporated porosome complex is shown. Note the spokes in the complex. The reconstituted complex at higher magnification is shown in b–d. Bar=100 nm. (From reference (42)).

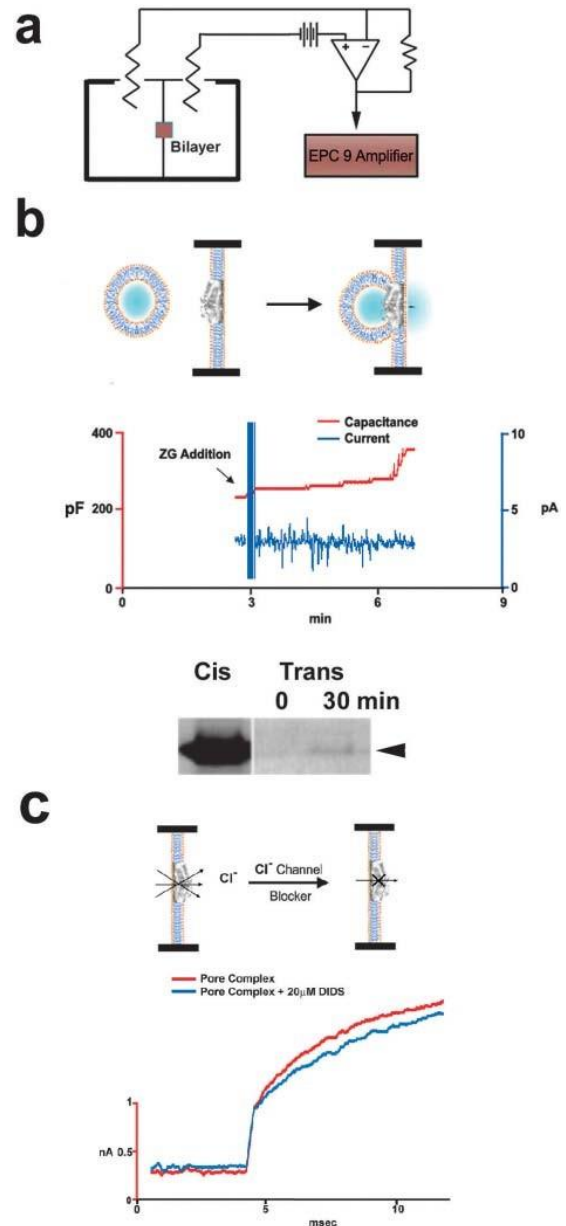


Figure 14. Functional reconstitution of the pancreatic porosome complex. (a) Schematic drawing of the EPC9 bilayer setup for electrophysiological measurements. (b) Zymogen granules (ZGs) added to the cis compartment (left) of the bilayer chamber fuse with the reconstituted porosomes, as demonstrated by the increase in capacitance (red trace) and current (blue trace) activities, and a concomitant time dependent release of amylase from the cis to the trans compartment of the bilayer chamber. The movement of amylase from the cis to the trans compartment in the EPC9 setup was determined by Western blot analysis of the contents in the cis and the trans chamber over time. (c) Electrical measurements in the presence and absence of chloride ion channel blocker DIDS, demonstrate the presence of chloride channels in association with the complex, and its requirement in porosome function. (From reference (42)).

Immunoisolation studies using SNAP-23 specific antibody on solubilized pancreatic plasma membrane fractions demonstrate the isolation of the porosome complex as assessed both structurally (**Figures 12 and 13**) and functionally (**Figure 14**) (42). Furthermore, immunochemical characterization of the pancreatic porosome complex demonstrates the presence of SNAP-23, syntaxin 2, actin, fodrin, vimentin, chloride channels CLC2 and CLC3, calcium channels $\beta 3$ and $\alpha 1c$, and the SNARE regulatory protein NSF, among other proteins (36,42). Transmission electron micrographs of pancreatic porosomes reconstituted into liposomes, exhibit a 150–200 nm cup-shaped basket-like morphology (**Figure 13**), similar to its native structure observed in cells and when co-isolated with ZG preparation (42). To test the functionality of the immunoisolated porosome complex, purified porosomes obtained from exocrine pancreas have been reconstituted in the lipid membrane of the EPC9 electrophysiological bilayer apparatus and exposed to isolated ZGs (**Figure 14**). Electrical activity of the porosome-reconstituted membrane, as well as the transport of vesicular contents from the *cis* to the *trans* compartments of the bilayer chambers, demonstrate that the lipid membrane-reconstituted porosomes are indeed functional. Thus, in the presence of calcium, isolated secretory vesicles dock and fuse to transfer intravesicular contents from the *cis* to the *trans* compartment of the bilayer chamber (**Figure 14**). ZGs fusion and content release through the reconstituted porosome is demonstrated by the increase in capacitance and conductance, and a time-dependent transport of the ZG enzyme amylase from *cis* to the *trans* compartment of the bilayer chamber measured using Western blot assays. Amylase is detected using immunoblot analysis of the buffer in the *cis* and *trans* compartments of the bilayer chambers. Chloride channel activity present in the porosome complex has been demonstrated to be critical to porosome function, since the chloride channel blocker DIDS is inhibitory to the function of the reconstituted porosome (**Figure 14**). Interestingly, recent studies (29) demonstrate the interaction between the cystic fibrosis transmembrane

conductance regulator (CFTR) and the porosome complex in human airways epithelia. This study implies that the CFTR chloride selective ion channel affects mucus composition and secretion through the porosome complex at the cell plasma membrane of the airways epithelia. Similarly, in cystic fibrosis, CFTR dysfunction is known to reduce secretory activity of pancreatic duct cells (26) which leads to blockage of the ductal system and eventual fibrosis of the entire gland. This is just one examples of diseases resulting from altered porosome-associated protein.

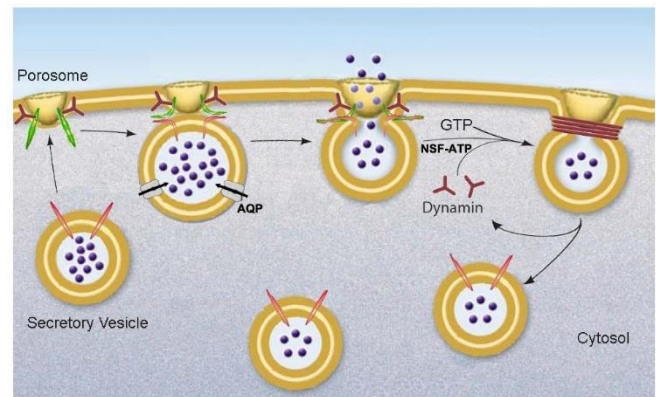


Figure 15. Schematic diagram depicting the transient docking and fusion of secretory vesicles at the porosome base in the cell plasma membrane, increase in turgor pressure of secretory vesicles via the entry of water and ions through water channels called aquaporins (AQP) and ion channels, expulsion of vesicular contents via the porosome to the outside, and the dissociation of the partially empty secretory vesicles from the porosome complex at the cell plasma membrane. (From reference (52)).

III. Porosome Proteins in Secretory Defects and Disease

Porosomes are composed of 30-40 proteins. The composition of proteins in porosomes from different tissue have been demonstrated to be similar, if not identical. Among porosome proteins of the exocrine pancreas, are the t-SNAREs (SNAP-23 and Syntaxin), actin, vimentin, α -fodrin, Ca^{2+} $\alpha 1c$ and Ca^{2+} $\beta 1c$ (36). Similarly, in the well characterized neuronal porosomes, actin, SNAREs, tubulin, and calcium and potassium transporters have also been reported (18, 36, 52).

It has long been established that actin is involved in neurotransmission (19) and our own studies demonstrate its role in secretion of amylase from the exocrine pancreas (62). Similar to the exocrine pancreas demonstrating the collapse of the porosome opening and loss of amylase secretion following exposure to the actin depolymerizing cytochalasin D (8), studies performed on neurons in presence of latrunculin A, also an actin depolymerizing agent, partially blocked neurotransmitter release at the pre-synaptic terminal of motor neurons (37). Actin b protein, a post-translational product of actb mRNA is important in formation of excitatory synapses, which is promoted by interaction of actb mRNA with Src associated in mitosis (Sam68 protein). Loss in Sam68 diminishes its interaction with actb mRNA leading to lower levels of synaptic actin b, which in turn leads to neurological disorders involved with abnormal synaptic transmissions (47). Although tubulin involvement in neurotransmission is not fully understood, its association with several synaptosomal proteins at the pre-synaptic membrane (44,45), suggests an important role in neurotransmission. Besides actin and tubulin, other important class of proteins identified in the neuronal porosome, are the membrane integrated ion-channel proteins that are important in maintaining cellular homeostasis. A good example is the alpha sub-unit 3 of Na^+/K^+ ATPase present in the porosome and plays a critical role in neurotransmission. Na^+/K^+ ATPase activity is known to be blocked by dihydroouabain (DHO) (38). Activation of Na^+/K^+ ATPase inhibits synaptic transmission, which results from the secretion of a pre-synaptic protein 'follistatin-like 1' which activates the alpha 1 subunit of the ATPase. Transient blocking of Na^+/K^+ ATPase pump using DHO result in an increase in both the amplitude and number of action potentials at the nerve terminal. Interestingly, Na^+/K^+ ATPase inhibition is calcium dependent and it has been demonstrated that increased intracellular calcium levels inhibit Na^+/K^+ ATPase, which increases excitability of neurons (63). Similarly, the porosome protein plasma membrane calcium ATPases (PMCA) is an important class of proteins known to be involved in

maintaining calcium homeostasis within cells including neurons (52). PMCA2 has been shown to co-localize in synaptosomes with synaptophysin (38). At the presynaptic membrane, Syntaxin-1 also a porosome protein, has been demonstrated to co-localize with PMCA2 and the glycine transporter 2 (GlyT2) that is found coupled to the Na^+/K^+ pump, suggesting the presence of a protein complex involved in neurotransmission (51-53). Similarly, deletion of PMCA2 generates an ataxic phenotype in mice, where the neurons possess prolonged hyperpolarized membrane, resulting from an increase in the basal levels of calcium within these neurons. Mutation in the PMCA2 encoding gene is known to result in homozygous deafwaddler mice (dfw/dfw) and they show high levels of calcium accumulation within their synaptic terminals. NAP-22, also known as BASP-1, is a protein found in the neuronal porosome complex. Due to its localization at the pre- and post-synaptic membranes and also in synaptic vesicles, it has been long speculated to be involved in synaptic transmission (38). NAP-22 is known to bind to the inner leaflet of lipid rafts suggesting interaction with cholesterol. Adenylyl cyclase associated protein-1 (CAP-1) is known to regulate actin polymerization and both actin and CAP-1 are present in the porosomal complex. In cells depleted of CAP-1 using RNAi, result in lamellipodia growth and F-actin accumulation along with other cytoskeletal abnormalities. In Alzheimer's, the levels of CNPase (2,3-cyclic nucleotide phosphodiesterase) and the heat shock protein 70 (HSP70), are found to increase while the levels of dihydropyrimidinase related protein-2 (DRP-2) decrease. Decreased levels of CNPase have been detected in the frontal and temporal cortex of patients with Alzheimer's disease and or Down's syndrome. Low CNPase levels have also been detected in post-mortem anterior frontal cortex in schizophrenic patients (38). Additionally, an allele that is associated with low levels of CNPase is also reported to be linked to schizophrenia (71). CNPase is also detected as a marker for oligodendroglia and myelin and several diseases associated with low levels of CNPase indicating low myelin on neurons (72). CNPase positive cells have been shown to

increase in corpus callosum of rats exposed to an enriched environment, meaning given to perform a task. Similarly, alterations in the levels of several of the SNARE proteins are associated with various neurological disorders. For instance, SNAP-25 and synaptophysin are significantly reduced in neurons of patients with Alzheimer's disease. Mice that are SNAP-25 (+/-) show disabled learning and memory and exhibit epileptic like seizures (38). Over expression of SNAP-25 also results in defects in cognitive function. Loss of SNAP-25 is also associated with Huntington's disease and a reduction in rabphilin 3a, another protein involved in vesicle docking and fusion at the presynaptic membrane. SNARE knockout mice are neonatally lethal and mice with a dominant mutation in SNAREs are known to develop ataxia and show impairment in vesicle recycling capability. Increase in synaptophysin levels along with SNAP-25 are also observed in Brodmann's area in the post-mortem brain of patients with bipolar disorder I. Protein levels of synaptotagmin and syntaxin 1 are highly upregulated in areas of cerebral ischemia, which are known to exhibit highly active levels of neurotransmission. Mutations in certain regions of the protein syntaxin 1A, such as Ca^{+2} channel-binding region is known to increase neurotransmitter release, which suggests that syntaxin 1A is involved in regulating Ca^{+2} channel function. A point mutation in syntaxin 1A is known to result in augmented release of neurotransmitters in models of the fruit fly *Drosophila melanogaster*. Synaptotagmin similar to syntaxin, has Ca^{+2} binding domains, and is known to form dimers and interact with syntaxin to form complexes in the presence of calcium (38). Binding of synaptotagmin to SNAP 25 is also calcium dependent (80,81). Reticulons are proteins which contribute to lipid membrane curvature and are found in the neuronal porosome complex. The involvement of reticulons with the porosome and diseases associated with their deregulation lend credence to the role of membrane curvature in regulation of synaptic vesicle fusion at the porosome complex. These studies reflect on the critical role of various neuronal porosome proteins in protein-protein, and protein-lipid interactions

within the porosome complex and in their participation in normal porosome-mediated neurotransmission at the nerve terminal and in disease. In addition to the above studies discussed on the involvement of porosome proteins in neurotransmission-related disease, recent morphological studies on the neuronal porosome complex have also shed light on both the health and disease status of the neuronal porosome complex as examined using high resolution EM (38). Ultrastructure of the neuronal porosome complex in rats subjected to continuous white noise that is relevant to the increasing random noise encountered by humans in today's environment, are known to provoke diverse effects on different brain regions such as the documented alteration in the length of the porosome complex. Constant exposure to such noise is further known to sabotages the development and normal function of audition, impair hearing, language acquisition, memory performance and other cognitive functions.

IV. Summary

In summary, these studies demonstrate how the power and scope of the AFM (5) enabled the discovery of the porosome, first in acinar cells of the exocrine pancreas (62,36,42), and later in other cell types including neurons (18,52). Porosomes are permanent supramolecular lipoprotein structures at the cell plasma membrane in pancreatic acinar cells, where membrane-bound secretory vesicles called ZGs transiently dock and fuse to release intravesicular contents from within cells to the outside. A schematic drawing of porosome-mediated fractional release of intravesicular contents during cell secretion is presented in **Figure 15**. As opposed to the complete merger of secretory vesicles at the cell plasma membrane (via an all or none mechanism), the porosome complex prevents secretory vesicle collapse at the cell plasma membrane during the secretory process, and provides precise regulation of intravesicular content release during cell secretion. Whether secretion involves the docking and fusion of a single vesicle or compound

exocytosis where a docked vesicle may involve a number of vesicles fused, the porosome would provide specificity and regulation of content release without compromising the integrity of the secretory vesicle membrane and the cell plasma membrane. In this porosome-mediated secretion, following fractional discharge of intra-vesicular contents, the partially empty vesicle may undergo several docking-fusion-release cycles until empty, prior to being recycled. However, in neurons, synaptic vesicles could be rapidly refilled via neurotransmitter transporters present at the vesicle membrane. A number of secretory defects and disease states are now recognized as a consequence of dysfunction of one or more porosome proteins (38). Further understanding of the molecular structure and regulation of the porosome complex will provide new and novel

therapeutic applications. The recent functional reconstitution of the insulin-secreting porosome complex in live beta cells of the endocrine pancreas, opens a window in the treatment of diabetes. To determine the distribution of constituent proteins within the complex, will require further studies using small angle X-ray solution scattering (48), chemical cross linking followed by mass spectrometry, immuno-EM, immuno-AFM, and single particle cryo electron tomography.

V. Acknowledgements

The work described in this manuscript was supported in part by grants from the NIH R01 DK56212 and NS39918 and NSF EB00303, CBET1066661 to BPJ.

VI. References

1. **Alexander S, Hellemans L, Marti O, Schneir J, Elings V, and Hansma PK.** An atomic resolution atomic force microscope implemented using an optical lever. *J Appl Physics* 65, 164–167, 1989.
2. **Almers W, and Tse FW.** Transmitter release from synapses: does a preassembled fusion pore initiate exocytosis? *Neuron*. 4: 813-818, 1990. [PMID: 1972885](#)
3. **Aravanis AM, Pyle JL, and Tsien RW.** Single synaptic vesicles fusing transiently and successively without loss of identity. *Nature* 423: 643–647, 2003. [PMID: 12789339](#)
4. **Bennett MK, Calakos N, and Scheller RH.** Syntaxin: A synaptic protein implicated in docking of synaptic vesicles at presynaptic active zones. *Science* 257:255-259, 1992. [PMID: 1321498](#)
5. **Binnig G, Quate CF, and Gerber CH.** Atomic force microscope. *Phys Rev Lett* 56, 930–933, 1986. [PMID: 10033323](#)
6. **Brunger AT, Weninger K, Bowen M, and Chu S.** Single-molecule studies of the neuronal SNARE fusion machinery. *Annu Rev Biochem* 78: 903–928, 2009. [PMID: 19489736](#)
7. **Ceccarelli B, Hurlbut WP, and Mauro A.** Turnover of transmitter and synaptic vesicles at the frog neuromuscular junction. *J Cell Biol* 57: 499-524, 1973. [PMID: 4348791](#)
8. **Chapman ER.** How does synaptotagmin trigger neurotransmitter release? *Annu Rev Biochem* 77: 615–641, 2008. [PMID: 18275379](#)
9. **Chen Z-H, Lee J-S, Shin L, Cho W-J, and Jena BP.** Involvement of β -adrenergic receptor in synaptic vesicle swelling and implication in neurotransmitter release. *J Cell Mol Med* 15: 572-576, 2011. [PMID: 20132410](#)
10. **Cho S-J, Cho J, and Jena BP.** Number of secretory vesicles remain unchanged following exocytosis. *Cell Biol Int* 26(1):29-33, 2002. [PMID: 11779218](#)
11. **Cho S-J, Jeftinija K, Glavaski A, Jeftinija S, Jena BP, and Anderson LL.** Structure and dynamics of the fusion pores in live GH-secreting cells revealed using atomic force microscopy. *Endocrinology* 143: 1144-1148, 2002. [PMID: 11861542](#)
12. **Cho S-J, Kelly M, Rognlien KT, Cho JA, Horber JKH, and Jena BP.** SNAREs in opposing bilayers interact in a circular array to form conducting pores. *Biophys J* 83: 2522-2527, 2002. [PMID: 12414686](#)
13. **Cho S-J, Quinn AS, Stromer MH, Dash S, Cho J, Taatjes DJ, and Jena BP.** Structure and dynamics of the fusion pore in live cells. *Cell Biol Int* 26: 35-42, 2002. [PMID: 11779219](#)
14. **Cho S-J, Sattar AKM, Jeong E-H, Satchi M, Cho J, Dash S, Mayes MS, Stromer MH, and Jena BP.** Aquaporin 1 regulates GTP-induced rapid gating of water in secretory vesicles. *Proc Natl Acad Sci USA* 99: 4720-4724, 2002. [PMID: 11917120](#)
15. **Cho S-J, Wakade A, Pappas GD, and Jena BP.** New structure involved in transient membrane fusion and

- exocytosis. *Ann N Y Acad Sci* 971: 254-256, 2002. [PMID: 12438127](#)
16. **Cho WJ, Lee J-S, Ren G, Zhang L, Shin L, Manke CW, Potoff J, Kotaria N, Zhvania MG, and Jena BP.** Membrane-directed molecular assembly of the neuronal SNARE complex. *J Cell Mol Med* 15: 31-37, 2011. [PMID: 20716122](#)
 17. **Cho W-J, Jeremic A, and Jena BP.** Size of supramolecular SNARE complex: membrane-directed self-assembly. *J Am Chem Soc* 127: 10156-10157, 2005. [PMID: 16028912](#)
 18. **Cho W-J, Jeremic A, Rognlien KT, Zhvania MG, Lazrshvili I, Tamar B, and Jena BP.** Structure, isolation, composition and reconstitution of the neuronal fusion pore. *Cell Biol Int* 28: 699-708, 2004. [PMID: 15516328](#)
 19. **Cole JC, Villa BR, and Wilkinson RS.** Disruption of actin impedes transmitter release in snake motor terminals. *J Physiol* 525(3): 579-586, 2000. [PMID: 10856113](#).
 20. **Cook JD, Cho WJ, Stemmler TL, and Jena BP.** Circular dichroism (CD) spectroscopy of the assembly and disassembly of SNAREs: the proteins involved in membrane fusion in cells. *Chem Phys Lett* 462: 6-9, 2008. [PMID: 19412345](#)
 21. **Craciun C, and Barbu-Tudoran L.** Identification of new structural elements within 'porosomes' of the exocrine pancreas: a detailed study using high-resolution electron microscopy. *Micron* 44: 137-142, 2013. [PMID: 22819153](#)
 22. **Diao J, Ishitsuka Y, and Bae WR.** Single-molecule FRET study of SNARE-mediated membrane fusion. *Biosci Rep* 31: 457-463, 2011. [PMID: 21919892](#)
 23. **Drescher DG, Cho WJ, and Drescher MJ.** Identification of the porosome complex in the hair cell. *Cell Biol Int Rep* 18: 31-34, 2011. [PMID: 22348194](#)
 24. **Elshennawy WW.** Image processing and numerical analysis approaches of porosome in mammalian pancreatic acinar cell. *J American Sci* 6: 835-843, 2011.
 25. **Fasshauer D, and Margittai M.** A Transient N-terminal interaction of SNAP-25 and syntaxin nucleates SNARE assembly. *J Biol Chem* 279: 7613-7621, 2004. [PMID: 14665625](#)
 26. **Gray MA, Winpenny JP, Verdon B, McAlroy H, and Argent BE.** Chloride channel and cystic fibrosis of the pancreas. *Biosci Rep* 15(6):531-541, 1995. [PMID: 9156582](#)
 27. **Hammel I, and Meilijson I.** Function suggests nano-structure: electrophysiology supports that granule membranes play dice. *J R Soc Interface* 9: 2516-2526, 2012. [PMID: 22628211](#)
 28. **Hörber JKH, and Miles MJ.** Scanning probe evolution in biology. *Science* 302, 1002-1005, 2003. [PMID: 14605360](#)
 29. **Hou X, Lewis KT, Wu Q, Wang S, Chen X, Flack A, Mao G, Taatjes DJ, Sun F, and Jena BP.** Proteome of the porosome complex in human airways epithelia: Interaction with the cystic fibrosis transmembrane conductance regulator (CFTR). *J Proteomics* 96:82-91, 2014. [PMID: 24220302](#)
 30. **Hui E, Johnson CP, Yao J, Dunning FM, and Chapman ER.** Synaptotagmin-mediated bending of the target membrane is a critical step in Ca²⁺-regulated fusion. *Cell* 138: 709-721, 2009. [PMID: 19703397](#)
 31. **Issa Z, Manke CW, Jena BP, and Potoff JJ.** Ca²⁺ bridging of apposed phospholipid bilayer *J Phys Chem* 114: 13249-13254, 2010. [PMID: 20836527](#)
 32. **Jahn R, and Scheller RH.** SNAREs—engines for membrane fusion. *Nature Rev Mol Cell Biol* 7: 631-643, 2006. [PMID: 16912714](#)
 33. **Japaridze NJ, Okuneva VG, Qsovreli MG, Surmava AG, Lordkipanidze TG, Kiladze MT, and Zhvania MG.** Hypokinetic stress and neuronal porosome complex in the rat brain: The electron microscopic study. *Micron* 43: 948-953, 2012. [PMID: 22571877](#)
 34. **Jena BP.** Porosome: the secretory portal. *Exp Biol Med* 237: 748-757, 2012. [PMID: 22859740](#)
 35. **Jena BP, Schneider SW, Geibel JP, Webster P, Oberleithner H, and Sritharan KC.** Gi regulation of secretory vesicle swelling examined by atomic force microscopy. *Proc Natl Acad Sci USA* 94: 13317-13322, 1997. [PMID: 9371843](#)
 36. **Jena BP, Cho S-J, Jeremic A, Stromer MH, and Abu-Hamdah R.** Structure and composition of the fusion pore. *Biophys J* 84: 1337-1343, 2003. [PMID: 12547814](#)
 37. **Jena BP.** Nano Cell Biology of Secretion: Imaging its Cellular and Molecular Underpinnings. *Springer Briefs in Biological Imaging* 1: 1-70, 2012.
 38. **Jena BP.** Cellular Nanomachines. Natures Engineered Marvels. *Springer Nature* 2020. ISBN: 9783030444952; DOI: [10.1007/978-3-030-44496-9](#).
 39. **Jeremic A, Cho W-J, and Jena BP.** Membrane fusion: what may transpire at the atomic level. *J Biol Phys Chem* 4: 139-142, 2004.
 40. **Jeremic A, Cho W-J, and Jena BP.** Involvement of water channels in synaptic vesicle swelling. *Exp Biol Med* 230: 674-680, 2005. [PMID: 16179736](#)
 41. **Jeremic A, Kelly M, Cho J-H, Cho S-J, Horber JKH, and Jena BP.** Calcium drives fusion of SNARE-apposed bilayers. *Cell Biol Int* 28: 19-31, 2004. [PMID: 14759765](#)

42. **Jeremic A, Kelly M, Cho S-J, Stromer MH, and Jena BP.** Reconstituted fusion pore. *Biophys J* 85: 2035-2043, 2003. [PMID: 12944316](#)
43. **Jeremic A, Quinn AS, Cho W-J, Taatjes DJ, and Jena BP.** Energy-dependent disassembly of self-assembled SNARE complex: observation at nanometer resolution using atomic force microscopy. *J Am Chem Soc* 128: 26-27, 2006. [PMID: 16390104](#)
44. **Kelly M, Cho W-J, Jeremic A, Abu-Hamdah R, and Jena BP.** Vesicle swelling regulates content expulsion during secretion. *Cell Biol Int* 28: 709-716, 2004. [PMID: 15516329](#)
45. **Khanna R, Zougman A, and Stanley EF.** A proteomic screen for presynaptic terminal N-type calcium channel (CaV2.2) binding partners. *J Biochem Mol Bio* 40: 302-314, 2007. [PMID: 17562281](#).
46. **Khanna R, Li Q, Bewersdorf J, and Stanley EF.** The presynaptic CaV2.2 channel-transmitter release site core complex. *Eur J Neurosci* 26: 547-559, 2007. [PMID: 17686036](#).
47. **Klein ME, Yount TJ, Castillo PE, and Jordan BA.** RNA-binding protein Sam68 controls synapse number and local beta-actin mRNA metabolism in dendrites. *Proc Natl Acad Sci USA* 110:3125-3130, 2013. [PMID: 23382180](#).
48. **Kovari LC, Brunzelle JS, Lewis KT, Cho WJ, Lee J-S, Taatjes DJ, and Jena BP.** X-ray solution structure of the native neuronal porosome-synaptic vesicle complex: Implication in neurotransmitter release. *Micron* 56: 37-43, 2014. [PMID: 24176623](#)
49. **Larina O, Bhat P, Pickett JA, Launikonis BS, Shah A, Kruger WA, Edwardson JM, and Thorn P.** Dynamic regulation of the large exocytotic fusion pore in pancreatic acinar cells. *Mol Biol Cell* 18(9):3502-3511, 2007. [PMID: 17596517](#)
50. **Lee J-S, Cho W-J, Shin L, and Jena BP.** Involvement of cholesterol in synaptic vesicle swelling. *Exp Biol Med* 235: 470-477, 2010. [PMID: 20407079](#)
51. **Lee J-S, Hou X, Bishop N, Wang S, Flack A, Cho WJ, Chen X, Mao G, Taatjes DJ, Sun F, Zhang K, and Jena BP.** Aquaporin-assisted and ER-mediated mitochondrial fission: a hypothesis. *Micron* 47: 50-58, 2013. [PMID: 23416165](#)
52. **Lee J-S, Jeremic A, Shin L, Cho WJ, Chen X, and Jena BP.** Neuronal Porosome proteome: Molecular dynamics and architecture. *Journal of Proteomics* 75: 3952-3962, 2012. [PMID: 22659300](#)
53. **Martens S, Kozlov MM, and McMahon HT.** How synaptotagmin promotes membrane fusion. *Science* 316: 1205-1208, 2007. [PMID: 17478680](#)
54. **Matsuno A, Itoh J, Mizutani A, Takekoshi S, Osamura RY, Okinaga H, Ide F, Miyawaki S, Uno T, Asano S, Tanaka J, Nakaguchi H, Sasaki M, and Murakami M.** Co-transfection of EYFP-GH and ECFP-rab3B in an experimental pituitary GH3 cell: a role of rab3B in secretion of GH through porosome. *Folia Histochem Cytobiol* 46, 419-421, 2008. [PMID: 19141391](#)
55. **Misura KM, Scheller RH, and Weis WI.** Three-dimensional structure of the neuronal-Sec1-syntaxin 1a complex. *Nature* 404: 355-362, 2000. [PMID: 10746715](#)
56. **Monck JR, and Fernandez JM.** The exocytotic fusion pore. *J Cell Biol* 119: 1395-1404, 1992. [PMID: 1469040](#)
57. **Okuneva VG, Japaridze ND, Kotaria NT, and Zhvania MG.** Neuronal porosome in the rat and cat brain. *Tsitologija* 54: 324-328, 2012. [PMID: 22724370](#)
58. **Oyler GA, Higgins GA, Hart RA, Battenberg E, Billingsley M, Bloom FE, and Wilson MC.** The identification of a novel synaptosomal-associated protein, SNAP-25, differentially expressed by neuronal subpopulations. *J Cell Biol* 109: 3039-3052, 1989. [PMID: 2592413](#)
59. **Paredes-Santos TC, de Souza W, and Attias M.** Dynamics and 3D organization of secretory organelles of *Toxoplasma Gondii*. *J Struct Biol* 177: 420-430, 2012. [PMID: 22155668](#)
60. **Pobbati AV, Stein A, and Fasshauer D.** N- to C-terminal SNARE complex assembly promotes rapid membrane fusion. *Science* 313: 673-676, 2006. [PMID: 16888141](#)
61. **Savigny P, Evans J, and McGarth KM.** Cell membrane structures during exocytosis. *Endocrinology* 148: 3863-3874, 2007. [PMID: 17494998](#)
62. **Schneider SW, Sritharan KC, Geibel JP, Oberleithner H, and Jena BP.** Surface dynamics in living acinar cells imaged by atomic force microscopy: identification of plasma membrane structures involved in exocytosis. *Proc Natl Acad Sci USA* 94: 316-321, 1997. [PMID: 8990206](#)
63. **Scuri R, Lombardo P, Cataldo E, Ristori C, and Brunelli M.** Inhibition of Na⁺/K⁺ ATPase potentiates synaptic transmission in tactile sensory neurons of the leech. *Eur J Neurosci* 25: 59-167, 2007. [PMID: 17241277](#).
64. **Shen J, Taresté DC, Paumet F, Rothman JE, and Melia TJ.** Selective activation of cognate SNAREpins by Sec1/Munc18 proteins. *Cell* 128: 183-195, 2007. [PMID: 17218264](#)
65. **Shin L, Basi N, Lee J-S, Cho W-J, Chen Z, Abu-Hamdah R, Oupicky D, and Jena BP.** Involvement of vH⁺-ATPase in synaptic vesicle swelling. *J Neurosci Res* 88: 95-101, 2010. [PMID: 19610106](#)
66. **Shin L, Cho W-J, Cook J, Stemmler T, and Jena BP.** Membrane lipids influence protein complex assembly-disassembly. *J Am Chem Soc* 132: 5596-5597, 2010. [PMID: 20373736](#)

67. **Shin W, Ge L, Arpino G, Villarreal SA, Hamid E, Liu H, Zhao WD, Wen PJ, Chiang HC, and Wu LG.** Visualization of membrane pore in live cells reveals a dynamic-pore theory governing fusion and endocytosis. *Cell*. 2018 May 3;173(4):934-945.e12. [PMID: 29606354](#).
68. **Siksou L, Rostaing P, Lechaire JP, Boudier T, Ohtsuka T, Fejtova A, Kao HT, Greengard P, Gundelfinger ED, Triller A, and Marty S.** Three-dimensional architecture of presynaptic terminal cytomatrix. *J Neurosci* 27: 6868–6877, 2007. [PMID: 17596435](#)
69. **Stein A, Weber G, Wahl MC, and Jahn R.** Helical extension of the neuronal SNARE complex into the membrane. *Nature* 460: 525–528, 2009. [PMID: 19571812](#)
70. **Südhof TC, and Rizo J.** Synaptic vesicle exocytosis. *Cold Spring Harb Perspect Biol* 3: a005637, 2011. [PMID: 22026965](#)
71. **Südhof TC, and Rothman JE.** Membrane fusion: grappling with SNARE and SM proteins. *Science* 323: 474–477, 2009. [PMID: 19164740](#)
72. **Südhof TC.** The synaptic vesicle cycle. *Annu Rev Neurosci* 27: 509–547, 2004. [PMID: 15217342](#).
73. **Sutton RB, Fasshauer D, Jahn R, and Brunger AT.** Crystal structure of a SNARE complex involved in synaptic exocytosis at 2.4 Å resolution. *Nature*. 395: 347–353, 1998. [PMID: 9759724](#)
74. **Taatjes DJ, Rand JH, and Jena BP.** Atomic force microscopy: high resolution dynamic imaging of cellular and molecular structure in health and disease. *J Cell Physiol* 228:1949-1955, 2013. [PMID: 23526453](#)
75. **Taraska JW, Perrais D, Ohara-Imaizumi M, Nagamatsu S, and Almers W.** Secretory granules are recaptured largely intact after stimulated exocytosis in cultured endocrine cells. *Proc Natl Acad Sci USA* 100: 2070–2075, 2003. [PMID: 12538853](#)
76. **Thorn P, Fogarty KE, and Parker I.** Zymogen granule exocytosis is characterized by long fusion pore openings and preservation of vesicle lipid identity. *Proc Natl Acad Sci USA* 101: 6774–6779, 2004. [PMID: 15090649](#)
77. **Trimble WS, Cowan DW, Scheller RH.** VAMP-1: A synaptic vesicle-associated integral membrane protein. *Proc Natl Acad Sci USA* 85: 4538-4542, 1988. [PMID: 3380805](#)
78. **Wang S, Lee J-S, Bishop N, Jeremic A, Cho WJ, Chen X, Mao G, Taatjes DJ, and Jena BP.** 3D organization and function of the cell: Golgi budding and vesicle biogenesis to docking at the porosome complex. *Histochem Cell Biol* 137: 703-718, 2012. [PMID: 22527693](#)
79. **Weber T, Zemelman BV, McNew JA, Westerman B, Gmachl M, Parlati F, Söllner TH, and Rothman, JE.** SNAREpins: minimal machinery for membrane fusion. *Cell* 92: 759-772, 1998. [PMID: 9529252](#)
80. **Wickner W, and Schekman R.** Membrane fusion. *Nature Struct Mol Biol* 15: 658–664, 2008. [PMID: 18618939](#)
81. **Yao J, Gaffaney JD, Kwon SE, and Chapman ER.** Doc2 is a Ca²⁺ sensor required for asynchronous neurotransmitter release. *Cell* 147: 666–677, 2011. [PMID: 22036572](#)
82. **Zhao D, Lulevich V, Liu F, and Liu G.** Applications of atomic force microscopy in biophysical chemistry. *J Phys Chem B* 114: 5971-5982, 2010. [PMID: 20405961](#)